PERGAMON

Deep-Sea Research I 46 (1999) 1565–1591

DEEP-SEA RESEARCH
PART I

The pattern of cross-slope depositional fluxes

M. Amin, J.M. Huthnance*

Proudman Oceanographic Laboratory, Bidston Observatory, Birkenhead, L43 7RA, UK

Received 31 July 1997; received in revised form 9 January 1998; accepted 29 May 1998

Abstract

A simple model with horizontal and vertical diffusivities and settling velocity is used to calculate expected distributions of suspended particulate matter in a section across the continental shelf and slope. Dependencies on the shelf and slope profile, diffusivities, settling velocity, cross-slope advection and boundary sources/sinks are explored. It is found that the strongest factors are relative values of diffusivities and settling velocity, and the distribution of sources and sinks – including bottom deposition or resuspension. The latter is the principal means whereby an increased concentration near the bottom is likely, and is suggested as the usual reason for increased deposition recorded by sediment traps nearer the bottom. Observed thin, near-horizontal intermediate nepheloid layers put bounds on the vertical diffusivity and settling velocity, e.g. O(10^{-4} m^2 s^{-1}, 10^{-5} m s^{-1}) over Goban Spur in OMEX.

1. Introduction

Exchanges between shelf seas and the deep ocean are of topical interest for global fluxes and budgets. There have been several recent studies of shelf-edge exchange, with particulate matter as a special interest in relation to questions of carbon export, deposition and burial (for example).

The Coastal Zone Transition Program took place off northern California (Brink and Cowles, 1991) in an area of seasonal upwelling and associated export of organic matter in near-surface filaments. Studies in San Pedro Basin, southern California, have emphasised depositional fluxes to sediment traps – a decrease offshore and increase downwards indicated an origin on the shelf or upper slope (Huh et al., 1990)

* Corresponding author. Fax: + 44-151-65 38 345.
E-mail address: jmh@ccms.ac.uk (J.M. Huthnance)

0967-0637/99/$ - see front matter
PII: S0967-0637(99)00020-5

supported by a (variable) lithogenic component in the fluxes (Thunell et al., 1994a,b). ECOMARGE in the Gulf of Lions (Monaco et al., 1990) found suspended particulate matter (SPM) transport along-shelf in a benthic nepheloid layer and export preferentially down canyons. SEEP-II in the Middle Atlantic Bight (Biscaye et al., 1994) and OMEX over Goban Spur southwest of Ireland are notable for measurements of SPM fluxes sufficient to suggest cross-slope patterns of distribution.

In SEEP-II, fluxes were recorded by sediment traps over the continental slope. Depositional fluxes increased downwards towards the sea bed. They also had maxima at mid-slope, near depths $\sim$ 400 m (south section), 1000 m (north section), where flow speeds were a minimum (Biscaye and Anderson, 1994; see Fig. 1a). It was suggested that a minimum in turbulence energy allowed particles to settle out of the water column, forming high depositional fluxes.

In OMEX, fluxes to traps over the slope showed an increase with depth at both locations (water depths 1450 m, 3660 m). The increase was especially marked at the latter in winter, suggesting a lateral source at mid-depth. Antia et al. (1999) cite the possibility of resuspended material in bottom nepheloid layers detaching to form intermediate nepheloid layers (INL) as previously observed at various depths along

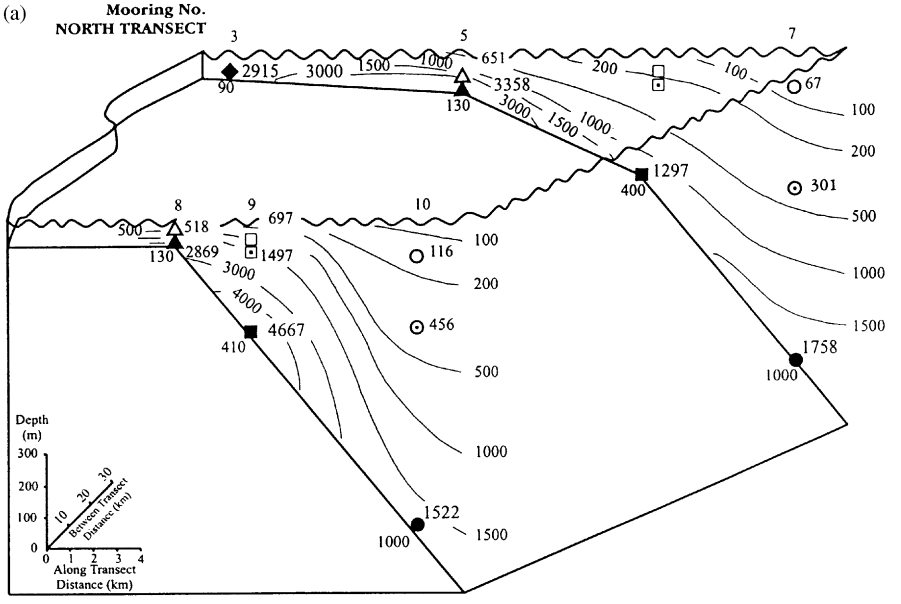

Fig. 1. Observed intermediate nepheloid layers: (a) From time-weighted average total mass flux (mg m^{-2} d^{-1}) of particulate matter collected by sediment traps during the course of the SEEP II experiment. Mooring numbers are shown above each set of symbols representing the traps on that mooring and the nominal water depth of the mooring is shown below (Biscaye and Anderson, 1994). (b) From super position of 14 profiles of percentage light transmission (trans) made over periods of 25 h at depth of 3512 db (3452 m) over the continental slope off the Porcupine Bank (Thorpe and White, 1988). (c) INLs from OMEX profiles.

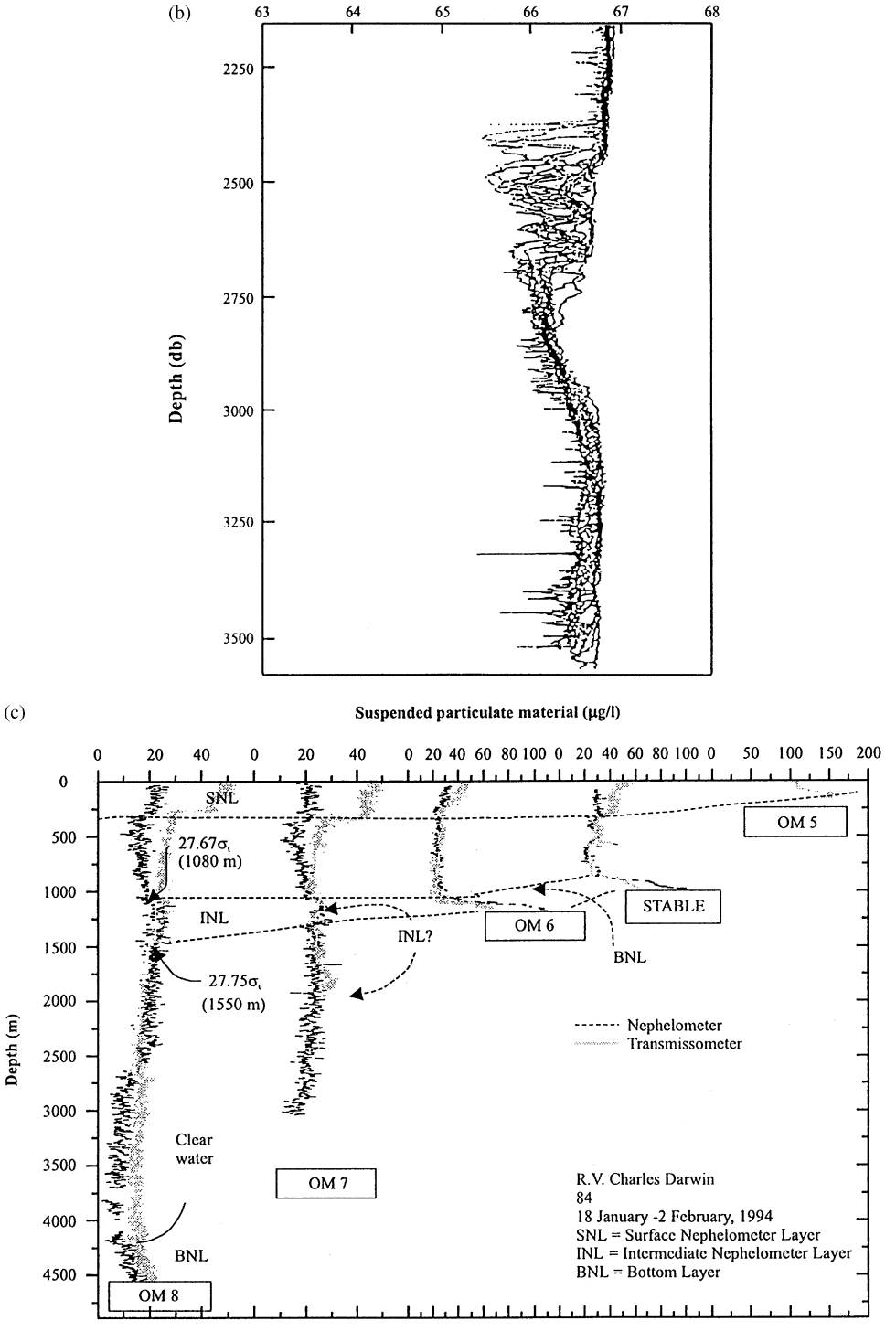

Fig. 1. (*continued*).

the slope to the north (Dickson and McCave, 1986; Thorpe and White, 1988; see Fig. 1b). Indeed, INL were observed in OMEX over Goban Spur, e.g. at depths of 500–1500 and 2200–3000 m (Antia et al., 1999; McCave et al., 1999; see Fig. 1c). A bottom nepheloid layer (BNL) was observed at CTD stations on the slope; thickness increased and intensity (particulate content) decreased down-slope to $\sim$2300 m; these trends, and material composition, suggest down-slope transport and a gradual settling of particles (van Weering et al., 1998). The observations are consistent with the idea of INL as detached BNL (from the area of most intense resuspension at $\sim$1200 m; McCave and Hall, 1996). Near-bed currents are locally or temporarily sufficient for this (van Weering et al., 1998). However, the INL appear to be transitory, and turbidity time-series from sediment trap moorings were not directly related to bulk deposition.

Cross-slope distributions of any dissolved or suspended constituent are controlled by advection, resulting from physical processes of large spatial scale, and by processes of small spatial scale unresolved by measurements. Effects of the latter are commonly aggregated as an "eddy diffusivity", which depends on the unresolved scales and processes, i.e. on the context and on the model using the "diffusivity". Empirically, as amply demonstrated in this paper and elsewhere, modelled distributions are sensitive to diffusivity values. Therefore, realistic diffusivity values are important to successful modelling, and observed distributions of marine constituents constrain the diffusivity values that models can assume. Potentially, any observed distribution constrains diffusivity values, most directly if the constituent is conservative and most distinctly if there are discrete sources. SPM may help in both ways.

Two-dimensional (2-D) models of the cross-slope section are common for various reasons: lack of information about along-slope variations; computing constraints associated with the need for fine cross-slope resolution or a complex set of modelled variables.

Accordingly, we investigate a minimal 2-D description of particulate fluxes over the slope, so that the results of assumptions about the origins of particles and the agents of their dispersion can be compared with observations as in SEEP-II and OMEX. After formulating the problem (Section 2) we carry out some analysis (Section 3) and a systematic set of parameter variations (Section 4) in comparison with a "control" case. The parameters varied are: shelf depth, shelf width, lateral "diffusivity", vertical "diffusivity" and settling velocity. Sources of SPM are also varied: surface source uniform over the shelf and slope; over the slope only; a coastal source; an additional source (resuspension) on the slope. In Section 5, direct application is made to the OMEX context to find constraints on the effective vertical diffusivity and settling velocity of particles in the observed INLs. The Section 6 discussion also includes some other contexts.

2. Formulation

Assuming along-shelf uniformity and no systematic advection in a cross-slope section, a transport equation (representing non-divergent flux in the steady state)

controls the concentration C of conservative suspended particulate matter (SPM):

$$0 = (K_H C_x)_x + (K_V C_z)_z + (W_S C)_z. \tag{2.1}$$

Here K_H, K_V are lateral and vertical diffusivities, W_S is the settling velocity of the SPM, x and z are Cartesian coordinates offshore and upwards; and subscripts denote differentiation. The downward depositional flux F_D is $W_S C + K_V C_z$. Of these two terms contributing to F_D, the first is dominant unless C varies substantially over the vertical scale K_V/W_S. The solutions show this to be the case typically only in relatively thin (K_V/W_S) layers near the bed. Thus, in general, the results will be shown in terms of C, which (for uniform W_S) will serve as an indicator for the depositional flux except in such thin layers. This point is exemplified later.

The bottom boundary condition deserves discussion, especially as results prove sensitive to it. Over a flat bottom, zero downward flux of sediment out of the water column is represented by $0 = F_D = W_S C + K_V C_z$. However, this implies resuspension of material arriving at the bottom. If the settling material (rate $W_S C$) is passively accepted on to the bottom (representing a downward flux out of the water column), then $W_S C = F_D$ or $K_V C_z = 0$. (The resulting condition $C_z = 0$ corresponds to a sea bed neither expelling nor attracting SPM).

Over a sloping bottom, the condition for the sediment flux $(-K_H C_x, -F_D)$ to have zero component along the direction $(-h_x, -1)$ out of the water column (normal to the bottom) is

$$0 = (-K_H C_x, -F_D)(-h_x, -1)/s.$$

However, this again implies resuspension of material arriving at the bottom. If the settling material is passively accepted on to the bottom, then the flux out of the water column, normal to the bottom, is $W_S C/s$ [in the above, s is the length of the vector $(-h_x, -1)$]. Hence

$$W_S C/s = (-K_H C_x, -F_D)(-h_x, -1)/s,$$

i.e.

$$0 = h_x K_H C_x + K_V C_z. \tag{2.2}$$

This is our condition for "passive acceptance" of settling material at the bottom. It corresponds to zero normal diffusive flux at the bottom, a condition that also applies within the sediment. Thus, (2.2) describes the settling flux $W_S C$ landing at the bottom without conversion to a diffusive flux. However, it is somewhat counter-intuitive in distorting constituent contours near the bed, as is well-known for isopycnals over a slope (Wunsch, 1970). The effect is illustrated in Fig. 4c and d, respectively, for contours that are near-vertical and near-horizontal in the interior away from the slope. The distortion occurs in a boundary layer against the slope of thickness K_H/W_S, K_V/W_S in x, z.

Referring to the argument before (2.2), the condition representing zero sediment flux out of the water column is

$$0 = h_x K_H C_x + K_V C_z + W_S C. \tag{2.3}$$

Eqs. (2.2) and (2.3) correspond to deposition rates $W_S C$, 0 respectively, i.e. to bottom shear-stress velocities $u^* = 0$, u_{crit} in the expression $W_S[1 - (u^*/u_{crit})^2]$ for depositional velocity commonly used as a bottom boundary condition in shallow shelf-sea models, e.g. Pohlmann and Puls (1995). (Bottom shear velocity $u^* > u_{crit}$ corresponds to erosion – an effective SPM source).

In Section 4, we explore effects of these alternative conditions (2.2) and (2.3) representing different degrees of deposition or resuspension.

3. Analyses

3.1. Offshelf decrease

Integrating (2.1) from a particular depth z up to the surface,

$$\left(- \int K_H C_x \, dz' = x - \text{flux} \right)_x = [W_S C + K_V C_z = \text{depositional flux}]_z^0. \tag{3.1}$$

For SPM of shelf origin, Eq. (3.1) (with both sides negative) clarifies the expectation that the x-flux will decrease offshore; the depositional flux takes material downwards out of the layer and increases downwards (from zero at the surface).

If the lower limit of integration is the bottom $z = -h$ where the bottom boundary condition (2.2) gives the depositional flux as $[W_S C]^{-h}$, then the inference is similar. For SPM of shelf origin, Eq. (3.1) (with both sides negative) relates a total x-flux decreasing offshore to deposition on the bottom (offset by any input at the surface).

3.2. Thin bottom boundary layer

We form an equation in x for the SPM integrated through a thin "benthic nepheloid layer" where the SPM is supposed to be concentrated, i.e. $C \approx 0$ just above ($z = T$). Integrating (2.1) from the bottom to $z = T$ and applying (2.2),

$$0 \approx - [W_S C]^{-h} + [K_H \{ (\int_{-h}^{T} C \, dz)_x - [h_x C]^{-h} \}]_x \tag{3.2}$$

as derived in Appendix A [Eq. (A.1) therein]. If we can define an effective layer thickness $\delta \equiv (\int_{-h}^{T} C \, dz)/[C]^{-h}$ then, as further discussed in Appendix A, this is effectively an equation for $[C]^{-h}$ and comparison may be made with a simple exponential decrease offshore at a rate $[W_S/K_H \delta]^{1/2}$. Thus, large settling velocity W_S and small diffusivities K_H and K_V will generally cause a benthic nepheloid layer to decay rapidly down-slope.

3.3. Elementary solutions

In uniform depth h, solutions of (2.1) having the form $X(x)Z(z)$ satisfy

$$(K_H X_x)_x / X = - [W_S Z_z + (K_V Z_z)_z]/Z, \tag{3.3}$$

where both sides are a constant that is expected to be positive, $\lambda^2 K_H$, offshore from sources. Thus, X behaves exponentially (with off-shelf decay) and Z sinusoidally. Natural boundary conditions for Z complement (2.2) and prescription of F_D at the upper boundary:

$$K_V Z_z = 0 \,(z = -h), \qquad W_S Z + K_V Z_z = 0 \quad (z = 0). \tag{3.4}$$

By (3.3), Z takes the form of one vertical structure mode:

$$Z = e^{-\alpha z}[P e^{\beta z} + Q e^{-\beta z}] \tag{3.5}$$

where

$$\alpha = W_S/2K_V, \beta = [W_S^2 - 4\lambda^2 K_H K_V]^{1/2}/2K_V.$$

In Appendix B it is concluded that a criterion for "large" or "small" depth is

$$h > \text{ or } h < \pi/2\alpha = \pi K_V/W_S.$$

This scale for h is a (bottom) boundary layer thickness as diffusion counters the tendency for SPM to settle. It is also found that there is an infinite sequence of modes with corresponding values $\lambda \sim (n-1)\pi(K_V/K_H)^{1/2}/h$ or $\lambda^2 K_H \sim (n-1)^2\pi^2 K_V/h^2$ for mode number n. These values λ are the rates of exponential decay (in X) offshelf.

In the Appendix B analysis, the physics is expressed in the factor $(\alpha^2 + \beta^2)$. The roots for $\lambda(K_V/K_H)^{-1/2}$ near $(n-1)\pi/h$ correspond to the sinuosoids necessary to complete the solution of Laplace's equation in the geometrical context, and are very inefficient when h is "large" corresponding to a relatively thin bottom boundary layer.

3.4. Simple solutions

For a flat shelf with a coastal source, the SPM concentration is a combination of the elementary solutions $X(x)Z(z)$ satisfying (3.3) et seq. There is offshore decay $\propto \exp(-\lambda_n x)$. The combination accords with the vertical structure of the input at the coast. Far enough offshore, only the lowest mode with slowest offshore decay remains. The decay rate corresponds to a vertical wavenumber (m in Appendix B) of order $\pi/2h$, i.e.

$$\lambda \sim \tfrac{1}{2}[W_S^2/(K_V K_H) + \pi^2 K_V/(h^2 K_H)]^{1/2}.$$

Such solutions also apply to the ocean with adjacent shelf input (regarding the continental slope as a "wall") or to an ocean with input from a sloping lateral boundary (the combination still accords with the vertical structure of the input, but the elementary solutions are not orthogonal along this boundary; the evaluation of coefficients has to be for all elementary modes simultaneously).

For uniform surface input F_D and horizontal uniformity in W_S and diffusivities, the unique solution is $C = F_D/W_S$. This remains valid over a sloping bottom.

For surface input $F_D\,(x < 0)$, zero $(x > 0)$ over uniform depth, there is anti-symmetry about the value $\frac{1}{2}F_D/W_S$ on $x = 0$. Then in $x > 0$ the solution is a combination of elementary modes decaying in x; the combination of vertical structures

matches $\frac{1}{2}F_D/W_S$ on $x = 0$. Thus

$$\tfrac{1}{2}F_D/W_S = \sum a_n Z_n \quad \text{where } a_n \int K_H E Z_n^2 \, dz = \tfrac{1}{2}F_D/W_S \int K_H E Z_n \, dz.$$

Here $E \equiv \exp(\int^z W_S/K_V)$ and the Sturm–Liouville equation $[K_V E^{-1}(ZE)_z]_z + \lambda^2 K_H Z = 0$ equivalent to (3.3) for Z gives the orthogonality relation $\int_{-h}^{0} K_H E Z_m Z_n \, dz = 0$ if $m \neq n$.

4. Numerical experiment

4.1. Reference case

Eq. (2.1) and boundary conditions (2.2) or (2.3) describing the transport of SPM with prescribed depositional flux over the surface are solved numerically using lowest order centred finite differences (Myint and Dibnath, 1987). The boundary conditions for open ocean and coastal points are assumed to be

$$\frac{\partial C}{\partial X} = -\lambda C, \quad \frac{\partial C}{\partial X} = 0,$$

respectively where λ is determined by (3.5) and (B.1).

Initial investigations were based on a rectangular grid of 400 km length in the horizontal (off-shore) direction and 2000 m in depth with a mesh spacing of $\Delta x =$ 5 km and $\Delta z = 10$ m. The lengths of shelf and slope in the 'reference' case were as shown in Fig. 2. The choice of grid length (400 km) in the horizontal direction is based on the criteria that model results, within the area under investigation (up to 200 km), should become stable. A further increase in the grid length should not have a significant effect on the distribution of SPM over and near the shelf. The coastal boundaries and bottom slope can be adjusted to make an experimental grid to represent any shelf, and the desired resolution can be obtained by changing the mesh size. By controlling the parameters K_H, K_V, W_S and F_D, a numerical scheme can help to generate conditions to replicate the real situation.

Reference values of parameters in the numerical simulation were $K_H = 10^3$, $K_V = 0.5 \times 10^{-2}$ and $W_S = 10^{-4}$ (m.k.s. units). $W_S = 10^{-4}$ m s^{-1} (or about 8 m/day) is chosen as a typical settling velocity for small particulate matter. There is evidence

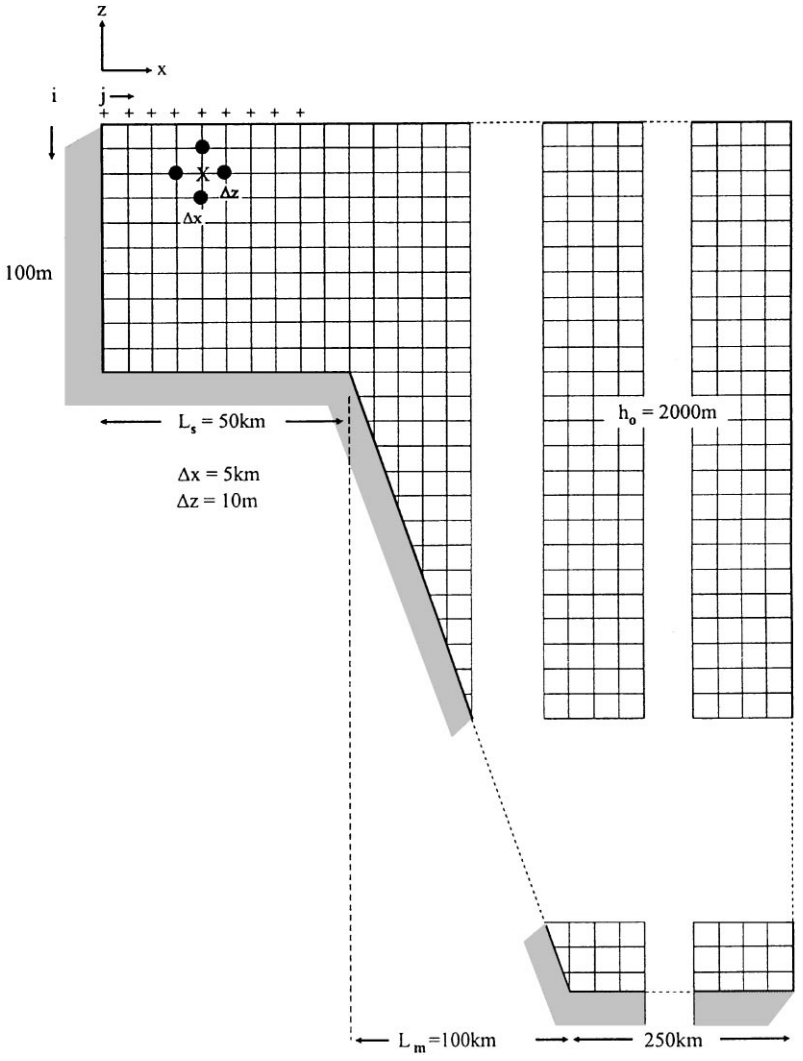

Fig. 2. Grid used in the finite difference scheme.

(reinforced by the present calculations) that some material falls much faster than this whilst the finest material in intermediate nepheloid layers falls more slowly. Hence, this choice of an intermediate reference value enables us, through variation of W_S, to explore the distinctive consequences of both fast and slow settling speeds. $K_H = 10^3\ m^2\ s^{-1}$ is a typical value used in coarse-resolution ocean general circulation models. $K_V = 5 \times 10^{-3}\ m^2\ s^{-1}$ is much larger than typical oceanic interior values but is often exceeded in the surface mixed layer and in shelf seas (Garrett and Gilbert,

1988). It corresponds to an Ekman layer depth scale of 10 m, for example. Moreover, the ratio K_V/W_S forms a vertical scale for any concentration of SPM near the bed; the choice of reference parameter values makes this scale 50 m to be visible in the results. We emphasise that the parameters are varied from these reference values to explore the effects of different values, in particular for application to the real case of Goban Spur.

Section 3 showed that a uniform SPM concentration and deposition results from a uniform flux at the surface, and material from the coast settles rapidly on the shallow shelf (if the SPM is supposed to settle without resuspension). Hence, we have chosen a spatially varying surface flux so that the spatial form of the solution can be explored in relation to parameter values. The particular form of surface flux (uniform over the shelf and slope, zero further offshore) is apparent in the corresponding surface concentrations (also discontinuous where the flux changes). The solution for this case over uniform depth is discussed in Section 3.4. Results for the concentration of SPM are shown in Fig. 3a. A lateral and downward dispersion of the SPM is the main feature of the distribution and there is no local mid-slope maximum or minimum concentration.

The truncation of the model at 400 km offshore was checked by a calculation with the model extended to 450 km. This resulted in no significant change in the calculated SPM field (Fig. 3b) confirming that the applied open-boundary condition satisfactorily represents continuation of the shelf and slope distribution into the wider ocean (for our limited source, over the shelf and slope only).

4.2. Parameter variations

To explore their effects on SPM distributions, variations from the reference case were made in turn to the diffusivities K_H, K_V, settling velocity W_S, shelf geometry and bottom boundary condition (representing degree of settling); cross-slope flow was also introduced, and source locations were varied.

Varying the parameter K_H shows that as its value is decreased in magnitude, vertical diffusion and settling velocity exert a greater influence in the transport of material. In this case the material moves in vertically oriented columns (Fig. 4a). If the parameter K_H is increased, there is an increase in the lateral transport of the material, and within the limited offshore extent of our computation, downward flow of material in the water column becomes small and the concentration of SPM decreases (Fig. 4b).

Increasing the value of W_S helps to bring more material downwards and a vertically oriented structure is formed (Fig. 4c). When the value of W_S is decreased, K_H becomes a dominating force and a horizontal structure is formed (Fig. 4d). Varying the vertical diffusivity has a similar effect on the distribution of SPM as that produced by variations in settling velocity W_S (Fig. 4e). However, adjustments are small in magnitude. It can also be seen that increasing the horizontal diffusivity has an effect on the concentration which is the inverse of that produced by increasing the vertical diffusivity and the settling velocity.

It is noted that convergence of the solution is fast when K_V and W_S are small, and K_H is larger; this is when diagonal elements of the numerical scheme's matrix are large in comparison with the off-diagonal elements.

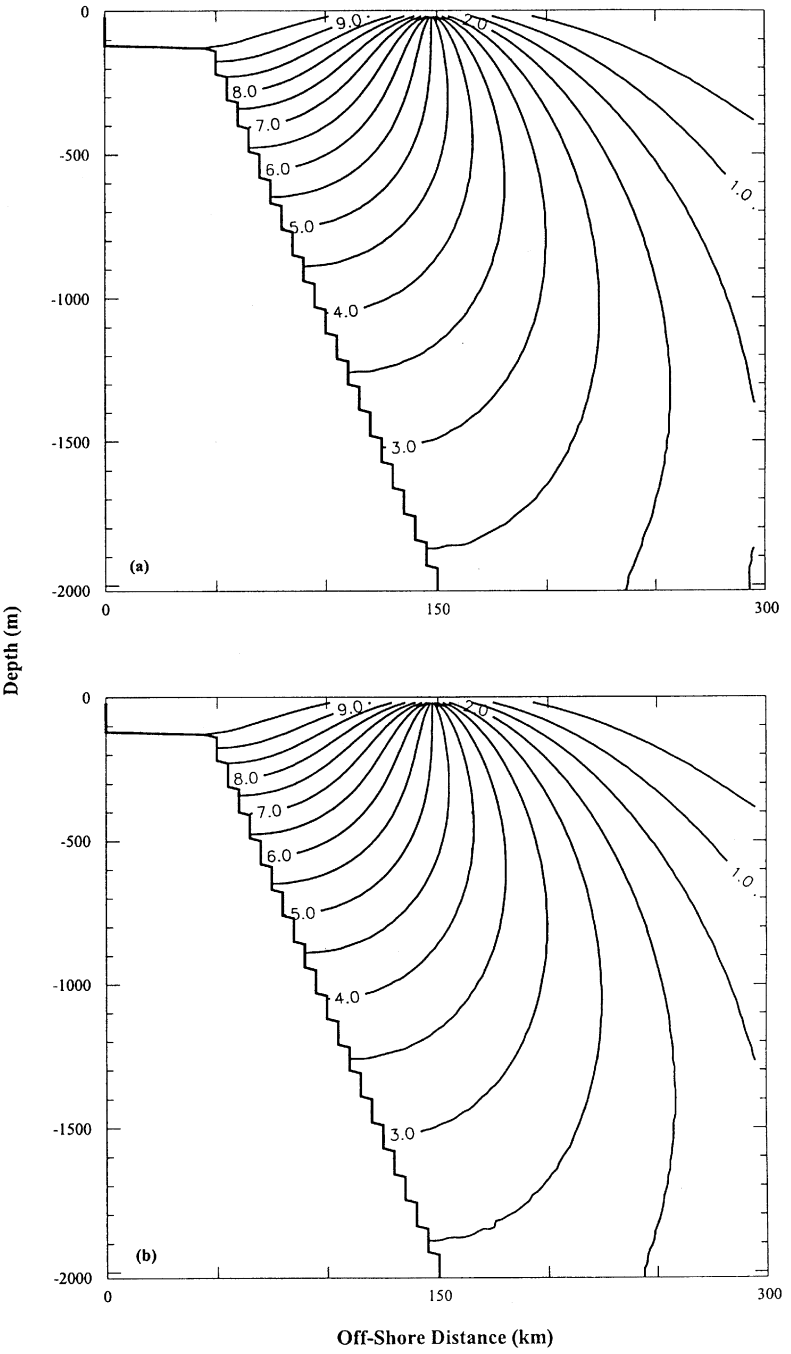

Fig. 3. Concentration of SPM when flux is through the surface over the shelf and reference values ($K_H = 10^3\ m^2\ s^{-1}$, $K_V = 0.5 \times 10^{-2}\ m^2\ s^{-1}$, $W_S = 10^{-4}\ m\ s^{-1}$, $F_D = 10^{-3}\ kg\ m^{-2}\ s^{-1}$) are used in the scheme: (a) when open boundary is at 400 km; (b) open boundary is at 450 km.

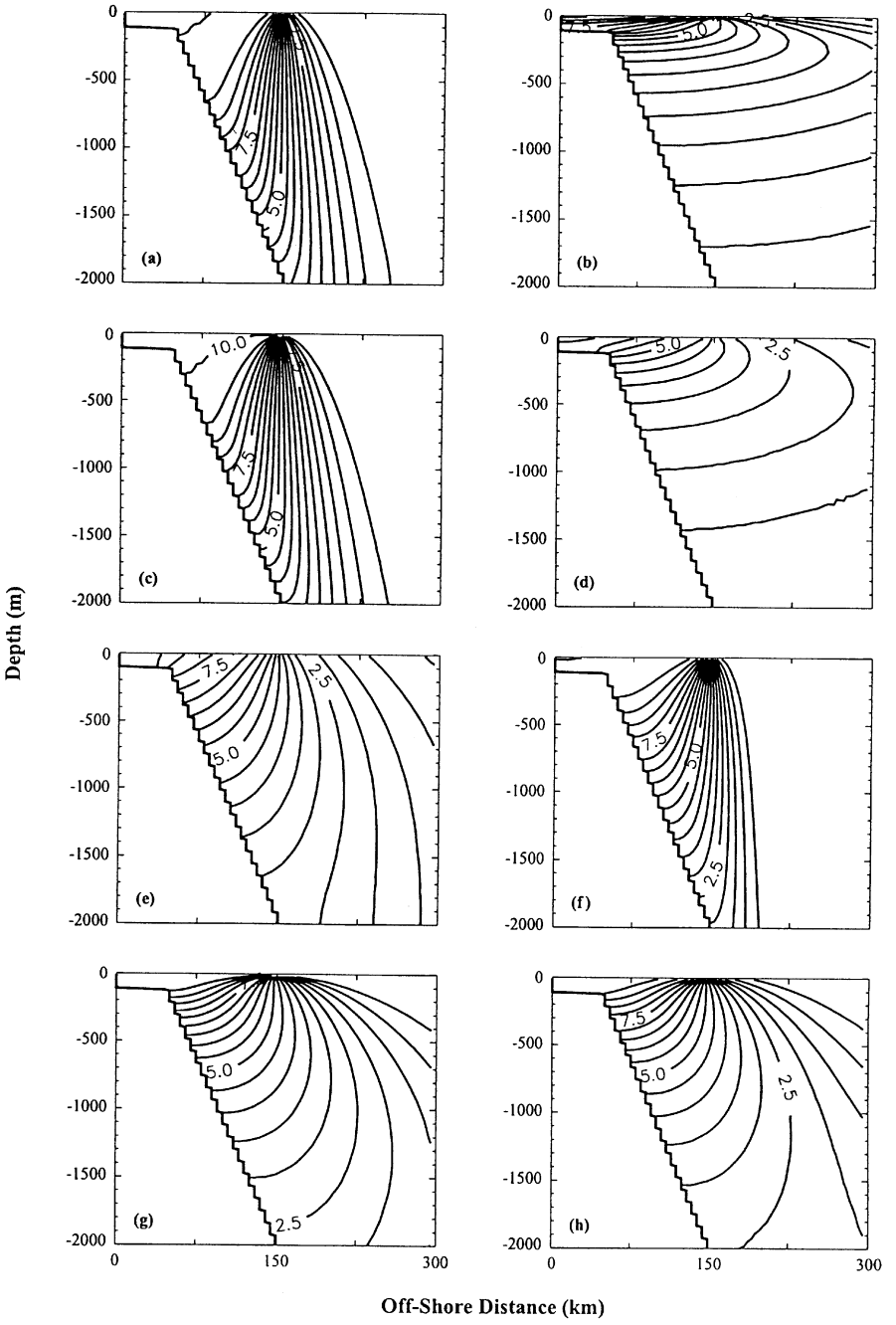

Fig. 4. Effect on the distribution of SPM due to: (a) decrease in horizontal diffusivity ($K_H = 10^2\ m^2\ s^{-1}$); (b) increase in horizontal diffusivity ($K_H = 10^4\ m^2\ s^{-1}$); (c) increase in settling velocity ($W_S = 10^{-3}\ ms^{-1}$); (d) decrease in settling velocity ($W_S = 10^{-5}\ m\ s^{-1}$); (e) K_V is increased to $0.05\ m^2\ s^{-1}$; (f) horizontal diffusivity is function of distance from the coast (4.2); (g) vertical diffusivity is function of distance from the coast; (h) vertical diffusivity is a function of Z, and prescribed as in (4.4).

In SEEP-II, there seemed to be a negative correlation between current speed (off-shelf and down slope) and depositional fluxes, in that greater fluxes were associated with regions of weaker currents. The regions of weaker currents can be considered as the areas where the turbulence energy and hence diffusivities K_H or K_V or both are small, allowing particles to settle out of the water column. To create such conditions, K_H and K_V are considered as functions of distance from coast to give minimal values of K_H and K_V at mid-depth such that

$$\begin{matrix}\hat{K}_H \\ \hat{K}_V\end{matrix} = f(x)\begin{bmatrix}K_H \\ K_V\end{bmatrix}, \tag{4.1}$$

in which

$$f(x) = \left[0.1 + 1.8\left|0.5 - \frac{x}{L}\right|\right]^2, \tag{4.2}$$

where $x = 0$ at the coast and L is the distance of the open boundary of the model from the coast. Alternatively, K_V can also be defined as a function of z such that

$$\hat{K}_V = g(z)K_V, \tag{4.3}$$

where

$$g(z) = [1 - 0.9e^{-(z-1000)^2/500^2}]. \tag{4.4}$$

The results when $\hat{K}_H$ and $\hat{K}_V$ vary according to Eq. (4.1) are shown in Fig. 4f and 4g, respectively. The changes in the concentration of SPM are significant when $\hat{K}_H$ varies as a function of x. In particular around $x = L/2$, where $\hat{K}_H$ becomes small, the horizontal movement of particles is virtually stopped. As K_V and W_S start dominating the transport, more material moves down and settles on the slope. Changes in $\hat{K}_V$ due to $f(x)$ have only a small effect on the distribution of SPM. When variations in $\hat{K}_V$ are depth dependent, some minor changes can be observed near the bottom (Fig. 4h).

Variations in the geometry of the shelf were also considered. Experiments suggest that concentration could increase at the edge of the shelf if its width is small (Fig. 5a) or if the shallow shelf itself slopes (Fig. 5b) as more material falls over the slope rather than on the shallow flat bottom. Although parameters and the geometry of the shelf can be adjusted to extend the on-shelf region of maximum concentration towards the shelf edge, this does not extend to a maximum on the mid-slope. Experiment with an increased slope shows that concentration increases in the lower-half of the water column as it becomes easier for SPM to move down.

Influence of the bottom boundary condition, Eq. (2.2), is examined by replacing it with (2.3). The new boundary condition has a remarkable effect on the concentration of SPM: it is high near the slope, and contours are almost parallel to the slope (Fig. 5c). When the new boundary condition is applied with an increased value of W_S, contours become parallel to the slope and the sector of maximum concentration is

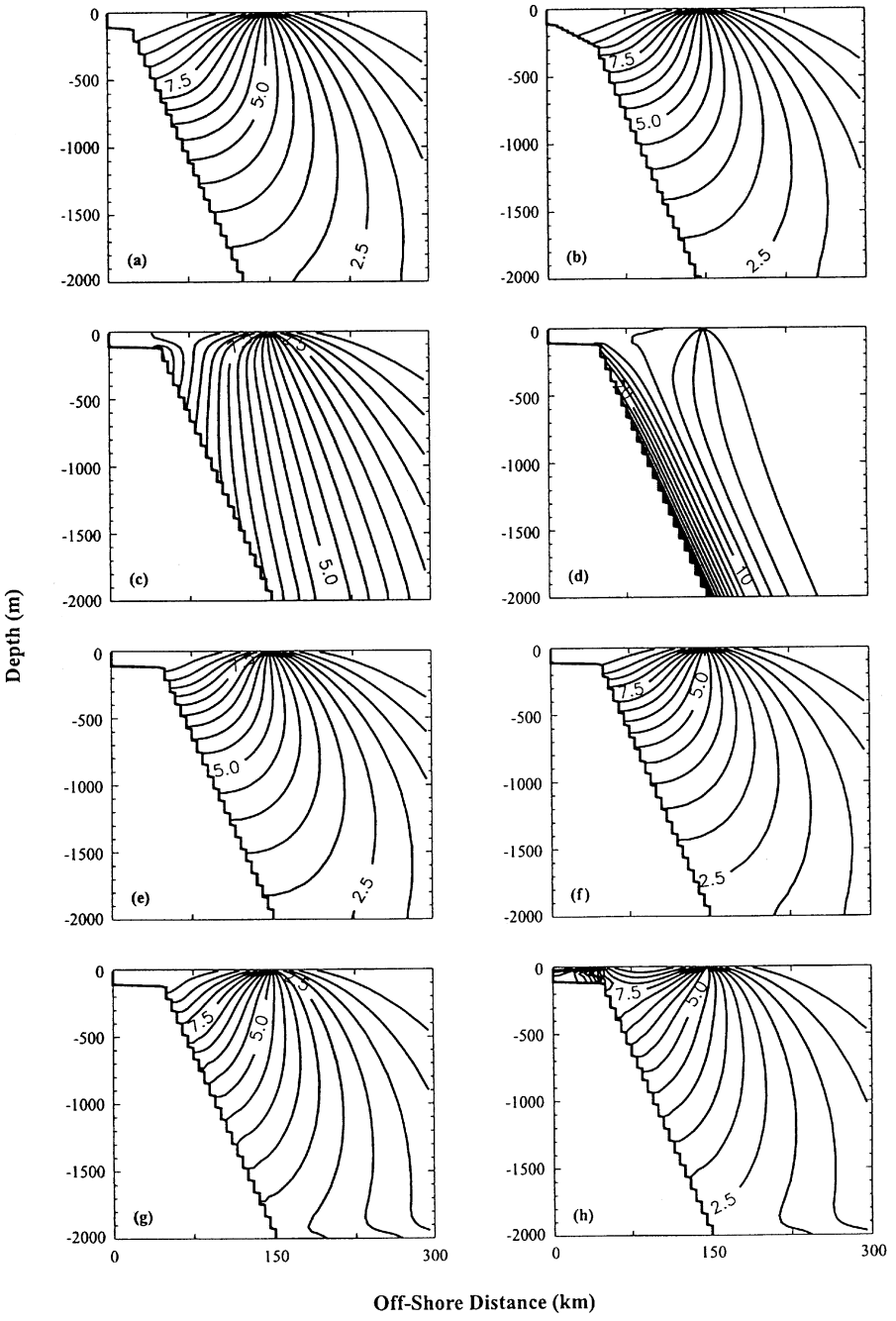

Fig. 5. SPM distribution with: (a) the shelf of reduced width; (b) the sloping bottom near the coast; (c) the bottom boundary condition as defined in Eq. (2.3); (d) same as in (c) but $W_S = 0.0005$ m s^{-1}; (e) advection as in Eq. (4.7) with $uh = 2$ m^2 s^{-1}; (f) $uh = -2$ m^2 s^{-1}; (g) on-shore flow as above and off-shore in bottom (50 m) boundary layer; (h) as in g and depositional flux is over the slope only.

shifted to the bottom (Fig. 5d). When the bottom boundary condition on the shelf slope is replaced by

$$\frac{\partial C}{\partial z} = 0$$

[for illustrative purposes only; see discussion of (2.2)] the pattern of distribution SPM is significantly changed (Fig. 6h).

The effect of cross-slope currents on the concentration of SPM is also simulated by adding advection terms to the diffusion equation (2.1) as

$$-[K_H C_x - uC]_x = [K_V C_z - wC]_z + (W_S C)_z, \tag{4.5}$$

where horizontal velocity u is specified in the form of a transport as

$$hu = Q$$

subject to the condition

$$u_x + w_z = 0, \tag{4.6}$$

$$w = \frac{z}{h}\frac{h_x}{h} Q \text{ any } z \tag{4.7}$$

In the numerical scheme these are also represented by lowest-order centred finite-differences. Since water transport carries SPM with it, some noticeable changes in the features of distribution of concentration are observed (Fig. 5e). Sections of high concentration move slightly down-slope and offshelf with off-shore flows $Q = 2\ \mathrm{m}^2/\mathrm{s}$. On-shore flow $Q = -2\ \mathrm{m}^2/\mathrm{s}$ produces slight changes in the reverse sense (Fig. 5f). Supposing that the water mass is conserved within the cross-slope section by an offshore transport in the bottom 50 m boundary layer (for example), matching on-shore transport above, gives an increased SPM concentration near the bottom (Fig. 5g). [Such a flow pattern has been suggested in the Middle Atlantic Bight. It is to be expected for prevalent poleward currents along the eastern ocean boundary and any associated bottom Ekman layer. A down-slope component of mean flow, 40 m above the bottom, was found in 660 m off NE Ireland during OMEX, for example (White and Bowyer, 1997). The value $Q = 2\ \mathrm{m}^2\ \mathrm{s}^{-1}$ is quite large for such a cross-slope exchange (Huthnance, 1995)]. When depositional flux on the surface is only above the slope, layers of high and low concentration are formed in the coastal water (Fig. 5h).

The position of the source of SPM has a very significant effect on the concentration. When depositional flux through the surface is only over the slope, the concentration has a maximum over the slope (Fig. 6a). Similarly, when an additional source is introduced at the mid-slope, a localised maximum appears there (Fig. 6b).

Some further tests were performed to examine the effects of the other conditions that may prevail. The influence of increased W_S on the SPM from a double source, at the surface and mid-slope, is shown in Fig. 6c and d. As increased W_S helps the downward transport of the material, on the shelf it tends to settle down quickly near the source. (Fig. 6e) gives the distribution of the concentration when the source is at

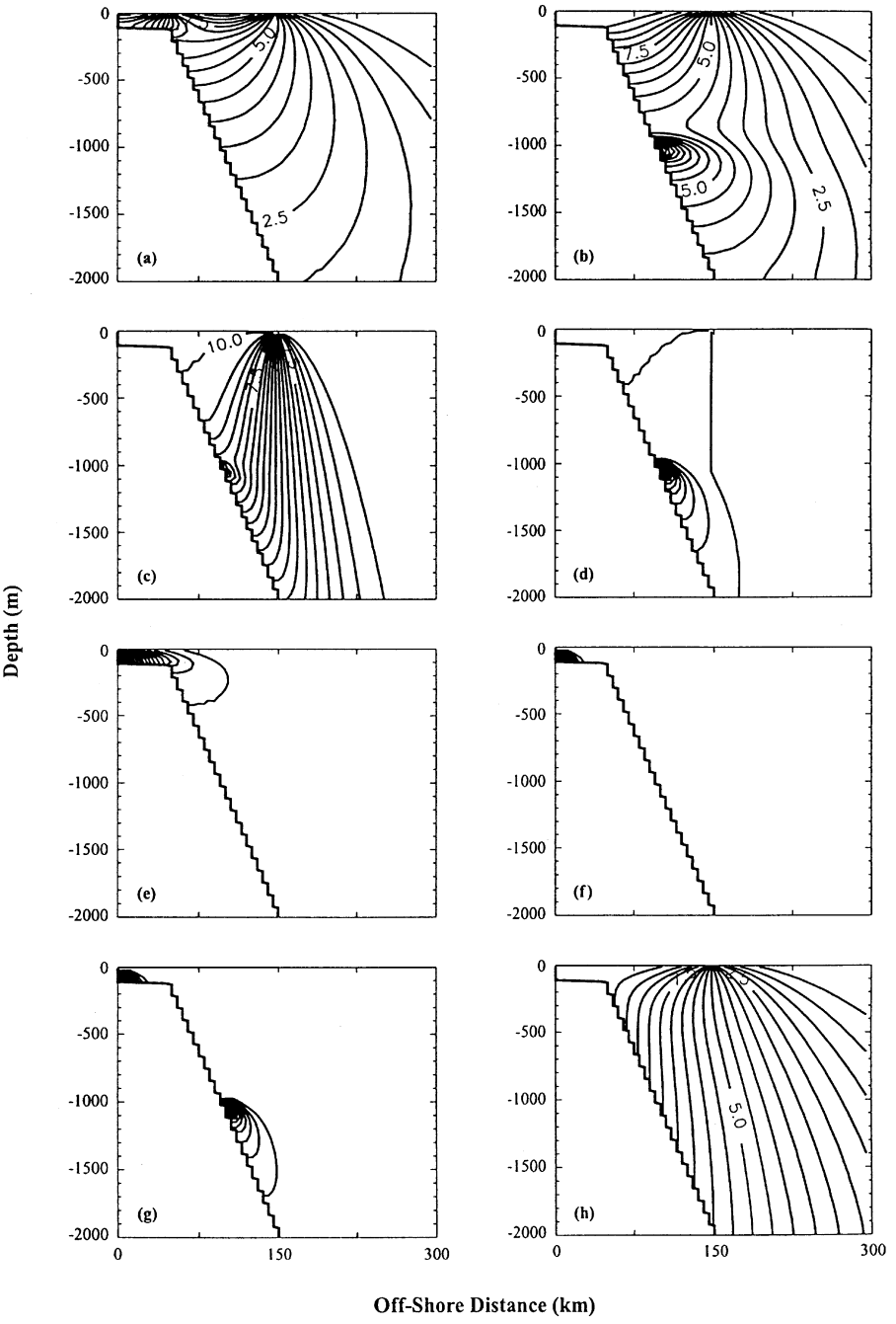

Fig. 6. Results from the numerical experiment when: (a) depositional flux over the slope only; (b) depositional flux as in the reference case plus a new source at mid-depth; (c) an additional source is introduced at mid-slope, $W_S = 10^{-3}$ m s^{-1} and $F_D = 10^{-2}$ kg m^{-2} s^{-1}; (d) same as in (c) but $F_D = 10^{-3}$ kg m^{-2} s^{-1}; (e) source is at the coast only; (f) source is at the coast and $W_S = 10^{-3}$ m s^{-1}; (g) sources are at the coast and mid-slope and $W_S = 10^{-3}$ m s^{-1}; (h) the boundary condition $\partial C/\partial z = 0$

the coast and the effect of increased W_S on it can be seen in Fig. 6f. It is also clear that material from the two sources does not mix together (Fig. 6g).

5. Application to Goban Spur

After experiments with the idealised shelf, the model is also used to explore the dispersive characteristics of SPM over the real shelf or a shelf of variable slope. For this purpose, the cross-sectional area is over the shelf along the line of OMEX measurements, where the x-axis in the off-shore direction is through (10°49.4′W, 49°29.5′N) and (12°49.5′W, 49°07.9′N). The mesh size is modified such that $\Delta x = 2$ km and $\Delta z = 20$ m, as the area covered is large and the slope is very steep. The results from the experiments with the idealised shelf grid suggest that the intermediate nepheloid layer is generated either by a secondary source on the slope or by a bottom boundary condition (2.3) that allows resuspension of the material at the sloping bottom. In view of these results from the idealised shelves, the model, when it is applied to the real shelf (Goban Spur), is initially driven by using the parameter values as in the reference case and applying the bottom boundary condition (2.3), which allows resuspension of material. The distribution of SPM is shown in Fig. 7a, where an INL can be seen at a depth of about 1200 m. The depth of the INL increases and its peak becomes flat as it moves away from the shelf. A second layer of high concentration of SPM is generated at a depth of 3750 m. Garrett and Gilbert (1988) have suggested that vertical diffusivity is of the order $1\text{–}4 \times 10^{-4}$ m^2 s^{-1}, which is smaller than its value in the reference case. When K_V is reduced to 4×10^{-4} m^2 s^{-1}, peaks of INLs are sharper as K_H starts dominating (Fig. 7b). A further decrease in the vertical diffusivity to 10^{-4} m^2 s^{-1} has increased the sharpness of the INL, and peaks are less enlongated in the downward direction (Fig. 7c). When the setting velocity is also reduced to 10^{-5} m s^{-1}, downward transport of SPM is very small and material stays in the upper layers (Fig. 7d).

A secondary source at the depth of 1200 m has generated a sharp peak, but again the downward transport is very limited (Fig. 7e). Corresponding flux contours are shown in Fig. 7f. A comparison of fluxes with the concentration shows that fluxes are almost proportional to the concentration of SPM. However, a careful examination shows that small differences exist in the regions where concentration contours are closely packed, i.e. $\partial C/\partial z$ is greater.

6. Discussion

6.1. General character of solutions

We have discussed solutions of (2.1). As an elliptic equation, its solutions are particularly constrained by values around the boundaries; internal maxima are unlikely according to the following argument. Taking (2.1) in the form of zero divergence

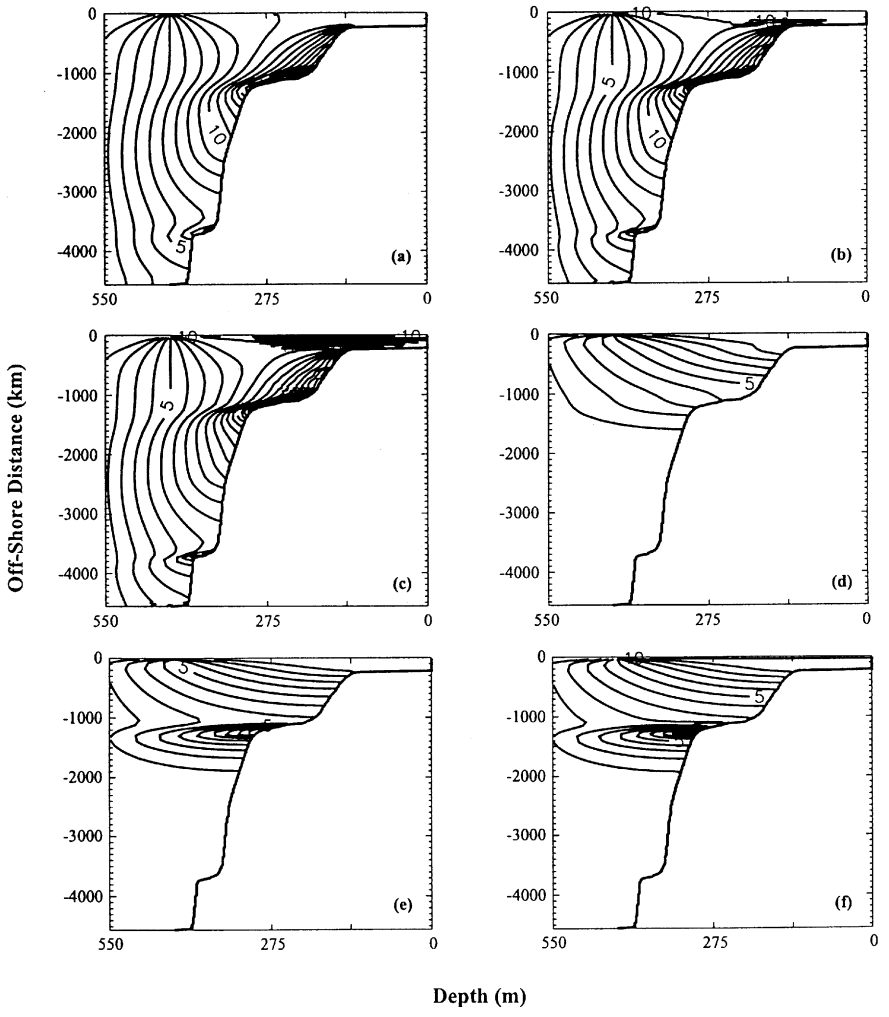

Fig. 7. Distribution of SPM over the real shelf (Goban Spur): (a) when reference values of parameters are used, (b) K_V is reduced 4×10^{-4} m^2 s^{-1}; (c) K_V is further decreased to 10^{-4} m^2 s^{-1}; (d) vertical diffusivity and settling velocity are 4×10^{-4} m^2 s^{-1} and 10^{-5} m s^{-1} respectively, and depositional flux through surface is 10^{-4}; (e) a second source is introduced on the slope and $K_V = 4\times10^{-4}$, $W_S = 10^{-5}$ m s^{-1} and $F_D = 10^{-4}$ kg m^{-2} s^{-1}; (f) same as *e* but contours of fluxes ($\times10^5$) are plotted instead of concentration C.

of the flux vector $(K_H C_x, K_V C_z + W_S C)$, we have

$$0 = \oint (K_H C_x, K_V C_z + W_S C)\cdot \mathbf{n}\, dl$$

taking the integral around any closed circuit in the (x, z) domain. In the absence of a settling velocity W_S, an interior maximum (meaning that the normal gradient of C is

negative away from the maximum) is impossible because C decreases in the direction of the normal $\mathbf{n}$, making the integral negative definite. Even with W_S, a maximum would require $(0, W_S C)\cdot\mathbf{n}$ to be greater where positive (over the upper sector of the integral loop) than where negative, to counteract the negative integral of the diffusive terms. This contradicts observations that C generally increases with proximity to the bottom. Thus, a priori, solutions of (2.1) are not amenable to internal maxima but are strongly affected by the applied boundary conditions (which reflect source and sink distributions, including deposition or resuspension at the bed).

The results strongly reflect this a priori behaviour. The relative values of K_H, K_V and W_S determine whether the distribution is "layered" (large K_H/L^2) or in "columns" (large K_V/D^2), where L and D are the lateral and vertical scales of the shelf-slope depth profile. K_V/W_S is the only absolute vertical scale formed "internally" by (2.1); in particular, it scales the height of any bottom boundary layer (notably with resuspension) where the solution adjusts to the bottom boundary condition. The general absence from the solutions of such a boundary layer, where the condition (2.2) is applied, indicates success of (2.2) in representing a passive boundary. Effects of different shelf-slope profiles were relatively modest.

Cross-slope advection of typical magnitude showed some effect where transport was concentrated in a bottom boundary layer (as in Fig. 4g, for example, where higher SPM values are advected down the slope and offshore). Particles advected at speed u will travel a distance uh/W_S before sinking through a depth h to the bottom, i.e. 20 km for our reference value $W_S = 10^{-4}\ \mathrm{m\ s^{-1}}$ and $uh = 2\ \mathrm{m^2\ s^{-1}}$ as in Section 4. A balance

$$[K_V C_z]_z = [uC]_x$$

between vertical diffusion and lateral advection determines another length scale $uh(h/K_V)$ over which advected particles will disperse vertically, e.g. 20 km for our reference value $K_V = 5\times10^{-3}\ \mathrm{m^2\ s^{-1}}$, $uh = 2\ \mathrm{m^2\ s^{-1}}$ and $h = 50$ m for a bottom boundary layer; 400 km for dispersion through the whole water column if $h = 1000$ m. Thus, the process of settling out dominates (is effective over a shorter distance of advection) if (as typically holds) $hW_S/K_V > 1$; then the advection distance uh/W_S applies.

The boundary conditions representing sources and sinks have a strong effect on the calculated distributions, as may be expected a priori. In all the calculations, the maximum SPM concentration is found at a source, i.e. where there is surface input, a specific coastal or bottom source, or the bottom boundary condition represents resuspension – in effect a source.

6.2. Comparison with observations

We consider three aspects of observations of SPM over the continental slope: downward increases in the material collected by sediment traps; benthic nepheloid layers; intermediate nepheloid layers.

Sediment traps in both SEEP (Biscaye and Anderson, 1994; see Fig. 1a) and OMEX (Antia et al., 1999) recorded downward increases in collected material over the

continental slope of the Middle Atlantic Bight and Goban Spur, respectively. However, we have seen that such an increase is most unlikely to be the result of an increased flux $F_D = W_S C + K_V C_z$ in which, outside a bottom boundary layer of thickness K_V/W_S, the first term is generally dominant and decreases downwards. In the case of a uniform flux input at the surface, F_D is uniform throughout. There is some doubt as to exactly what flux a sediment trap records: in fact not F_D, for if one considers a bottom source of fine sediment, F_D is negative whereas trap records are necessarily positive. These considerations suggest that the observed downward increases may be attributed to either resuspension at the bed or lateral input from some additional source (most obviously from the shelf or slope above, possibly by resuspension). In the case of OMEX, a generally alongslope flow but decreasing (tidal) energy levels along the slope suggest the possibility of a decreasing along-slope SPM flux.

Benthic nepheloid layers were found in both ECOMARGE (Monaco et al., 1990) and OMEX (van Weering et al., 1998). The application of the present model to the Goban Spur context of OMEX (as well as in the idealised geometry of Section 4) shows increased near-bed concentrations of SPM when the resuspension boundary condition (2.3) is applied, but not otherwise. The analysis of Section 3 also suggested off-shelf decay of any concentrated bottom layer of SPM, if the material all settles on the sea bed. This suggests that resuspension is a prerequisite for a benthic nepheloid layer. The OMEX application also shows the layer much more distinctly in the sectors of small bottom slope. Against a steeper slope h_x, a benthic nepheloid layer thickness $d = K_V/W_S$ implies lateral gradients of SPM (scale d/h_x), which are subject to lateral diffusion K_H and only sustainable if $K_H/(d/h_x)^2 < K_V/d^2$, i.e. $h_x < (K_V/K_H)^{1/2}$.

Intermediate nepheloid layers were seen by Hickey et al. (1986) around Quinalt Canyon, off Porcupine Bank (Thorpe and White, 1988; Figs. 2 and 3) and in OMEX (McCave and Hall, 1996; Fig. 1c). They appear in the application of the present model to the OMEX context if W_S and K_V are small (Fig. 8). The model also suggests that they depend on resuspension or a more specific source, and are favoured by the extensive "plateau" in the continental slope formed by Goban Spur. Small W_S sustains the layer in the water column rather than falling to the bed. Small K_V allows the SPM to remain in a relatively thin layer rather than dispersing throughout the water column. In each case, "small" is relative to K_H, as solutions retain the same form when W_S, K_V and K_H are all multiplied by the same arbitrary factor. In the time L^2/K_H for offshore displacement L, the SPM should not fall to the bottom: $h/W_S > L^2/K_H$ or $W_S < K_H h/L^{-2}$. Similarly $K_V < K_H(h/L)^2$. Even with K_H as large as $10^3\ m^2\ s^{-1}$ (as used in the OMEX application) the results show K_V limited to a small multiple of $10^{-4}\ m^2\ s^{-1}$ and W_S to $10^{-5}\ m\ s^{-1}$ (< 1 m per day) for an intermediate nepheloid layer. This implies vertical diffusion corresponding to oceanic interior values away from shelf seas and boundary mixing, and a fine particle content settling much more slowly than observed for the spring bloom collected in sediment traps.

For the benthic and intermediate nepheloid layers found in OMEX, where the additional SPM concentrations appear to be comparable with the "background" values, resuspension (rather than any specific extra source) can suffice to supply the layers.

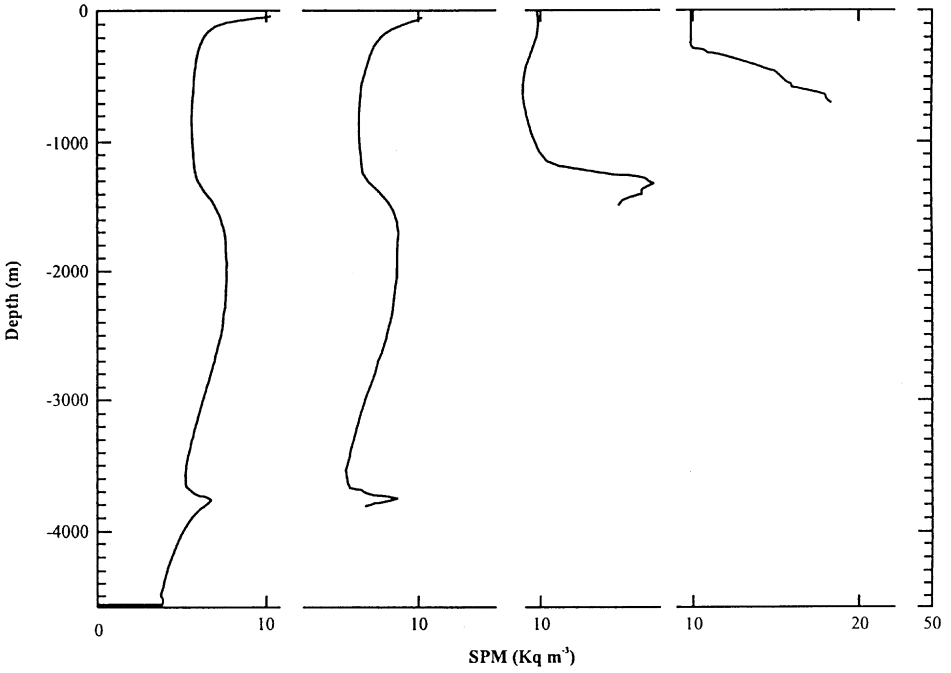

Fig. 8. Depth profiles of SPM concentration (kg m^{-3}) computed using the present model with parameter values as in Fig. 6b and water depth is shown on each plot.

6.3. *Critique of the model*

The model used here is (i) two-dimensional and (ii) steady.

A three-dimensional model would be required for more accurate simulations of SPM distributions affected by along-slope variations. Causes of along-slope variations include topography, flow fields and specific sources of SPM (perhaps related to the other two factors). For example, canyons may be the "preferred" location of downslope SPM transport, as found by ECOMARGE in the Gulf of Lions (Monaco et al., 1990). Instability of along-slope flow in upwelling contexts may result in offshelf filaments of water with more organic SPM than the non-upwelled water between, as found by the Coastal Zone Transition Program off northern California (Brink and Cowles, 1991).

A time-dependent model would be required for more accurate simulations of SPM distributions affected by the various sources of time dependence. There is seasonality in patterns of currents and in the favourability of conditions for production of organic SPM. Tides follow a spring-neap cycle, which may be influential for turbulence and stratification. Weather and diurnal or semi-diurnal tidal cycles may give strong short-term changes in currents, turbulence and stratification, possibly with large SPM

resuspension "events" Such effects of the weather may also control the exact timing of a relatively rapid bloom generating organic SPM.

As well as unresolved processes of small spatial scale, effects of along-slope variations and time dependence are also implicitly aggregated in the 2-D steady model as contributions to the eddy diffusivities. Shear-dispersion contributed by oscillatory (e.g. tidal) currents is a particularly effective case in point (e.g. Prandle, 1984; Huthnance, 1995). A representation as sources might be possible in some cases; if along-slope flow convergence brings SPM into the cross-section, for example; then divergent flow within the cross-section is also implied. At sufficiently large scales, along-slope (y) variations may not contribute significantly to the advective-diffusive balance, i.e. $(K_H C_y)_y \ll (K_H C_x)_x$. Similarly, the cross-slope distribution may be *quasi*-steady in its adjustment to conditions varying on time-scales long compared with the advective–diffusive time-scales h/W_S, h^2/K_V, L^2/K_H.

Hitherto, the best-measured cross-slope distributions of SPM have not been accompanied by much information on along-slope divergence, and time dependence is at best as given by sequential trap samples. Therefore, a 2-D steady model corresponds reasonably in sophistication with the data available for comparison. (The introduction gives additional motivation in relation to other 2-D cross-section models.)

Throughout, we have expressed results as SPM concentrations, more easily conceptualised than the flux F_D. As mentioned, the two are closely related by the factor W_S provided that vertical gradients C_z are small, i.e. the vertical scale of SPM variation is large compared with K_V/W_S. This small scale is manifested in our solutions only close to the bottom boundary and generally only where there is a source or resuspension of SPM. Hence, in practice, the results are expressed in a form illustrating F_D except in these limited contexts.

7. Conclusions

The strongest factors influencing SPM distributions over the slope are the relative values of effective lateral diffusivity, vertical diffusivity and settling velocity W_S. If L and H are the lateral and vertical scales of the depth profile, then large (small) K_H/L^2 relative to K_V/H^2 gives a layered (columnar) distribution. K_V/W_S scales the height of any near-bed layer, notably with resuspension. If K_V/W_S is small relative to water depths, as is typically true, then the depositional flux is dominated by $W_S C$ – distributed like C – in most of the water column.

Intermediate nepheloid layers are similarly constrained to sufficiently small $W_S < K_H h/L^2$ and $K_V < K_H(h/L)^2$. In the OMEX context, this means $W_S = O(10^{-5}\,\mathrm{m\,s^{-1}})$ or very fine particles and $K_V = O(10^{-4}\,\mathrm{m^2\,s^{-1}})$ typical of oceanic interior mixing (as opposed to the shelf or slope boundaries).

Geometrical factors such as relative shelf and slope width, and a sloping rather than a flat shelf, proved to be relatively modest in effect. The above scalings appear to predominate.

Advection also has a relatively modest effect for typical cross-slope exchange velocities, if $W_S = 10^{-4}\,\mathrm{m\,s^{-1}}$ as in our reference case. If $hW_S/K_V > 1$, then settling

out will dominate vertical dispersion and limit an advection distance to uh/W_S. This was much less than the scale of lateral dispersion in most of our calculations.

The surface "source" distribution and degree of sea-bed resuspension or particular sources are very influential on distributions. In particular, observed downward increases in flux to sediment traps are most obviously attributable to resuspension at the bed or to lateral convergence of SPM flux. Moreover, resuspension (or a specific bottom source) appears to be a prerequisite for a benthic nepheloid layer, which is favoured over sectors of small bottom slope.

The sensitivity of results to effective diffusivities, settling velocity and sources of particulates implies that this model (or others) cannot be used for predicting SPM distributions unless these quantities are well known (or the model incorporates the physical processes needed to predict them). Rather, as illustrated herein, the model may be used to infer clear evidence about diffusivities, settling velocity and sources from observed SPM distributions.

Acknowledgements

This work was supported by the EU through the MAST programme, contract MAS2-CT93-0069 (Ocean Margin Exchange – OMEX). We thank the referees for constructive comments.

Appendix A. Thin bottom boundary layer, Section 3.2

Integrating (2.1) through the layer and using (2.2),

$$\begin{aligned} 0 &= [W_S C + K_V C_z]_{-h}^{T} + \left(\int_{-h}^{T} K_H C_x \mathrm{d}z\right)_x - [T_x K_H C_x]^T - [h_x K_H C_x]^{-h} \\ &\approx -[W_S C]^{-h} + \left(\int_{-h}^{T} K_H C_x \mathrm{d}z\right)_x \\ &= -[W_S C]^{-h} + \left[K_H\left(\int_{-h}^{T} C \,\mathrm{d}z\right)_x - [h_x C]^{-h}\right]_x \end{aligned} \tag{A.1}$$

if $(K_H)_z = 0$. We need to close this by relating $[C]^{-h}$ to $\hat{C} \equiv \int_{-h}^{T} C \,\mathrm{d}z$. For this purpose we regard z as the coordinate *normal* to the *gently* sloping bottom; derivatives in z greatly exceed down-slope derivatives in the thin layer (supposed to vary relatively slowly down-slope):

$$W_S C_z + (K_V C_z)_z \approx 0,$$

i.e. $W_S C + K_V C_z = F_D$ independent of z.

Let

$$C = F_D/W_S \quad + C_c$$

(particular solution) (complementary function)

where

$$W_S C_C + K_V C_{Cz} = 0.$$

Then

$$C_C = C' \exp\left(- \int^z W_S/K_V \, dz' \right).$$

Our assumption of a confined bottom layer implies that $F_D = 0$ (above the layer). Hence

$$C = [C]^{-h} \exp\left(- \int_{-h}^z W_S/K_V \, dz' \right).$$

Then, e.g.,

K_V uniform:
$$\hat{C} = [C]^{-h} \int_{-h}^T \exp(- (z + h) W_S/K_V) \, dz$$
$$= [C]^{-h} K_V/W_S.$$

$K_V = \kappa u_* (z + h + z_0)$:

$$\hat{C} = [C]^{-h} \int_{-h}^T \exp\left(- \int_{-h}^z W_S/\kappa u_* (z' + h + z_0) dz' \right) dz$$
$$= [C]^{-h} \kappa u_* z_0/W_S.$$

Hence (A.1) becomes

$$0 = (K_H \hat{C}_x)_x - (K_H h_x \hat{C}/\delta)_x - W_S \hat{C}/\delta$$

or

$$0 = [K_H \hat{E} (\delta C/\hat{E})_x]_x - W_S C, \tag{A.2}$$

where $\delta \equiv \hat{C}/[C]^{-h}$ is the effective layer thickness (e.g. $\kappa u_* z_0/W_S$ or K_V/W_S),

$$\hat{E} \equiv \exp \int^x h_x/\delta \, dx.$$

We consider the form of solutions of the Sturm–Liouville (A.2). They are non-oscillatory because $W_S > 0$. Hence $K_H \hat{E} (\hat{C}/\hat{E})_x$ increases in x; it must be positive if anywhere $(\hat{C}/\hat{E})_x \geqslant 0$. However, solutions $\hat{C}$ with $(\hat{C}/\hat{E})_x \geqslant 0$ at least increase like $\hat{E}$ as

$x \to \infty$, which is unacceptable for shelf or slope sources of SPM. Therefore we require $(\hat{C}/\hat{E})_x < 0$. Hence C decreases eventually offshore in the ocean.

The transformation $\xi = \int^x (K_H \hat{E})^{-1}$, $D = \delta C/\hat{E}$ in (A.2) gives

$$0 = D_{\xi\xi} - [K_H W_S \hat{E}^2/\delta]D. \tag{A.3}$$

We compare D with the solution D^f of an analogous equation with constant coefficients:

$$0 = D^f_{\xi\xi} - [K_H W_S \hat{E}^2/\delta]^f D^f \tag{A.3′}$$

From $\int^\xi [D(\text{A.3}') - D^f(\text{A.3})]\,\mathrm{d}\xi$,

$$0 = [DD^f_\xi - D^f D_\xi] + \int^\xi DD^f W_S (K_H \hat{E}^2/\delta - K_H \hat{E}^2/\delta|^f)\,\mathrm{d}\xi,$$

i.e.

$$(D^f)^2 (D/D^f)_\xi = \int^\xi DD^f W_S (K_H \hat{E}^2/\delta - K_H \hat{E}^2/\delta|^f)\,\mathrm{d}\xi.$$

Because D (a constituent concentration), D^f (a simple exponential decay offshore satisfying (A.3′)) and W_S are all positive, (D/D^f) increases in ξ while $(K_H \hat{E}^2/\delta - K_H \hat{E}^2/\delta|^f) > 0$, indeed the increase in (D/D^f) becomes more rapid in ξ. Compared with a simple exponential decay offshore, therefore, an increase in $\delta C/\hat{E}$ is favoured by large $K_H \hat{E}^2/\delta$.

Appendix B. Offshore decay rates for elementary solutions, Section 3.3

In the notation of Section 3.3, by (3.4)

$$0 = W_S(P + Q) + K_V[-\alpha(P + Q) + \beta(P - Q)],$$

and

$$0 = K_V[(\beta - \alpha)P\mathrm{e}^{-\beta h} - (\beta + \alpha)Q\mathrm{e}^{\beta h}].$$

For non-zero solutions, the matrix of coefficients for P and Q must have zero determinant; i.e.

$$-2\alpha = (\alpha^2 + \beta^2)\tanh(\beta h)/\beta.$$

As λ increases from 0, α is constant, β decreases and $\tanh(\beta h)/\beta$ increases; all are positive until $\beta = 0$ so that all roots are in $\beta^2 < 0$, i.e. β is imaginary = im:

$$m = [4\lambda^2 K_H K_V - W_S^2]^{1/2}/2K_V$$

and

$$-2\alpha = (\alpha^2 - m^2)\tan(mh)/m. \tag{B.1}$$

As m increases from 0 (for λ continuing to increase), the left-hand side of (B.1) remains negative and the right-hand side positive until $mh = \pi/2$ or $m = \alpha$. Thus

$$h > \text{or } h < \pi/2\alpha = \pi K_V/W_S$$

is a criterion for "large" or "small" depth. This scale for h is a (bottom) boundary layer thickness as diffusion counters the tendency for SPM to settle.

For large h, $\tan(mh)$ changes sign, both sides are negative and as m continues to increase both $(\alpha^2 - m^2)$ and $\tan(mh)/m$ decrease towards zero (the latter from $-\infty$). There is a root before the first zero, i.e. in $m < \min(\pi/h, \alpha)$. Because $\tan(mh)/m$ cycles between $-\infty$ and $+\infty$ at intervals π/h, there are successive roots in each of these intervals. In one interval $[(n - \frac{1}{2})\pi/h, (n + \frac{1}{2})\pi/h]$, $(\alpha^2 - m^2)$ also has a zero and there are two roots. Subsequently, $(\alpha^2 - m^2)$ becomes large and negative and the nth root is just greater than $(n - 1)\pi/h$. Thus, values for large λ are $(n - 1)\pi(K_V/K_H)^{1/2}/h$, or $(n - 1)^2\pi^2 K_V/h^2$ for $\lambda^2 K_H$.

For small h, $(\alpha^2 - m^2)$ changes sign, both sides are negative and as m continues to increase both $(\alpha^2 - m^2)$ and $\tan(mh)/m$ increase in size (the latter towards ∞ at $mh = \pi/2$) so that there is a root in $m < \pi/2h$. Subsequently, $\tan(mh)/m$ cycles between $-\infty$ and $+\infty$ in each interval $[(n - \frac{1}{2})\pi/h, (n + \frac{1}{2})\pi/h]$ so that there are successive roots n just greater than $(n - 1)\pi/h$. Again, values for large λ are $(n - 1)\pi(K_V/K_H)^{1/2}/h$, or $(n - 1)^2\pi^2 K_V/h^2$ for $\lambda^2 K_H$.

References

Antia, A.N., von Bodungen, B., Peinert, R., 1999. Particle flux across the Mid-European continental margin: Deep-Sea Research, in press.

Biscaye, P.E., Anderson, R.F., 1994. Fluxes of particulate matter on the slope of the southern Middle Atlantic Bight: SEEP II. Deep-Sea Research II 41, 459–509.

Biscaye, P.E., Flagg, C.N., Falkowski, P.G., 1994. The Shelf Edge Exchange Processes experiment, SEEP-II: an introduction to hypotheses, results and conclusions. Deep-Sea Research II 41, 231–252.

Brink, K.H., Cowles, T.J., 1991. The coastal transition zone program. Journal of Geophysical Research 96, 14637–14647.

Dickson, R.R., McCave, I.N., 1986. Nepheloid layers on the continental slope west of Porcupine Bank. Deep-Sea Research 33, 791–818.

Garrett, C., Gilbert, D., 1988. Estimates of vertical mixing by internal waves reflected off a sloping bottom. In: Small-Scale Turbulence and Mixing in the Ocean, Proceedings of the 14th International Liège Colloquium on Hydrodynamics, Elsevier Oceanography Series, Vol. 46. Elsevier, Amsterdam, pp. 405–423.

Hickey, B.M., Baker, E.T., Kachel, N., 1986. Suspended particle movement in and around Quinalt submarine canyon. Marine Geology 71, 35–83.

Huh, C.-A., Small, L.F., Niemnil, S., Finney, B.P., Hickey, B.M., Kachel, N.B., Gorsline, D.S., Williams, P.M., 1990. Sedimentation dynamics in the Santa Monica – San Pedro Basin of Los Angeles: radiochemical, sediment trap and transmissometer studies. Continental Shelf Research 10, 137–164.

Huthnance, J.M., 1995. Circulation, exchange and water masses at the ocean margin: the role of physical processes at the shelf edge. Progress in Oceanography 35, 353–431.

McCave, I.N., Hall, I., 1996. Transport and accumulation fluxes of sediments at the shelf edge and slope of NW Europe, 48°–50°N. Ocean Margin Exchange Final Report E1-55.

McCave, I.N., Hall, I.R. Antía. A., Chan, L., Dehairs, F., Lampitt, R.S., Thomsen, L., van Weoring. T.C.E., Wollast, R., 1999. Sources, distribution, composition and flux of particulate material on the

European margin 47°–50°N, a synthesis of results from the OMEXI program. Deep-Sea Research, submitted.

Monaco, A., Biscaye, P.E., Soyer, J., Pocklington, R., Heussner, S., 1990. Particle fluxes and ecosystem response on a continental margin: the 1985–1988 Mediterranean ECOMARGE experiment. Continental Shelf Research 10, 809–839.

Myint, U.T., Debnath, L., 1987. Partial Differential Equating for Scientist and Engineers third ed. PRT Prentice-Hall Inc., Inglewood Cliff, NJ, p. 554.

Pohlmann, T., Puls, W., 1995. Currents and transport in water. In: Sündermann, J. (Ed.), Circulation and Contaminant Fluxes in the North Sea. Springer, Heidelberg, pp. 345–402.

Prandle, D., 1984. A modelling study of the mixing of ^{137}Cs in the seas of the European continental shelf. Philosophical Transactions of the Royal Society of London A 310, 407–436.

Thorpe, S.A., White, M., 1988. A deep intermediate nepheloid layer. Deep-Sea Research 35, 1665–1671.

Thunell, R.C., Moore, W.S., Dumond, J., Pilskaln, C.H., 1994a. Elemental and isotopic fluxes in the Southern California Bight: a time series sediment trap study in the San Pedro Basin. Journal of Geophysical Research 99, 875–889.

Thunell, R.C., Pilskaln, C.H., Tappe, E., Sautter, L.R., 1994b. Temporal variability in sediment fluxes in the San Pedro Basin, Southern California Bight. Continental Shelf Research 14, 333–352.

van Weering, T.C.E., Hall, I., De Stigter, H., McCave, I.N., Thomsen, L., 1998. Sediment transport and BNL dynamics at Goban Spur. Recent sediments, sediment accumulation and carbon burial at Goban Spur. Progress in Oceanography 42, 5–35.

White, M., Bowyer, P., 1997. The shelf-edge current north-west of Ireland. Annales Geophysica 15, 1076–1083.

Wunsch, C., 1970. On oceanic boundary mixing. Deep-Sea Research 17, 293–301.